SAE 2023-91-47

Effects of oxygenate and aromatic content on engine-out aldehyde emissions from pure, binary, and ternary mixtures of ethanol, toluene, and iso-octane

Varun Shankar, Felix Leach*
Department of Engineering Science, University of Oxford, Oxford, United Kingdom

ABSTRACT

Sustainable fuel components, such as ethanol, can be blended into gasoline to help reduce fossil fuel consumption. Aldehydes are both observed emissions and major intermediates in the oxidation of gasoline/ethanol fuel mixtures and are solely attributed to the fuel's alcohol content.

This study aims to evaluate the direct impact of toluene, iso-octane, and ethanol on engine-out formaldehyde and acetaldehyde emissions. A single-cylinder direct injection spark ignition engine was run at low speed and load conditions with varying equivalence ratios. The emissions are measured using a FTIR.

The aldehyde emissions from pure ethanol are ten- and five-times greater than pure toluene and iso-octane, respectively. Greater formaldehyde than acetaldehyde is found for iso-octane and toluene and vice versa for ethanol. The addition of 25 %vol of toluene to ethanol halves the average aldehyde emissions due to toluene suppressing effects. In the ternary mixtures with fixed ethanol content, the higher toluene concentration mixture led to lower average aldehyde emissions.

INTRODUCTION

To aid the reduction of fossil fuel consumption, ethanol, a prominent sustainable fuel, is blended in different ratios into gasoline [1]. The blending of 10% (by volume) of ethanol with a gasoline blendstock is the norm for spark ignition (SI) engines in the United States, United Kingdom, and part of European Union's (EU's) renewable energy directive [2, 3]. This proportion is increasing, for example, India has announced an E20 (20% by volume ethanol) blending mandate by 2025 [4]. Ethanol has been extensively used worldwide as a renewable fuel for three primary reasons. Firstly, it can be produced from renewable sources thus reducing the life cycle greenhouse gas (GHG) emissions with widely-studied and established processes [5]. Secondly, ethanol addition to gasoline enables knock resistance in SI engines, allowing for higher compression ratios and boosted intake pressure thus improving engine efficiency [6]. Thirdly, the addition of ethanol to gasoline has also been found to reduce the emissions of carbon monoxide (CO), tailpipe particulate matter (PM), and unburned hydrocarbons (UHC) [7, 8].

However, Yang *et al.* [9] found that blending up to 20 % (by volume) of ethanol with gasoline led to a statistically significant increase in aldehyde, specifically acetaldehyde, emissions. Formaldehyde (HCHO) and acetaldehyde (CH_3CHO) are the two most abundant aldehydes in ambient air. A rise in the ambient concentration of aldehydes can affect the atmospheric chemistry leading to the increased formation of the ozone and secondary pollutants [10]. The International Agency for Research on Cancer (IARC) classifies the pollutants into groups that define formaldehyde and acetaldehyde to be carcinogenic and probably carcinogenic, respectively [11]. Jacobson *et al.* [12] were able to associate the increased usage of high ethanol content fuels with cancer and mortality in the USA.

Ethanol is a well-studied precursor of aldehydes and the effect of mixing different concentrations of ethanol in gasoline has been extensively explored. For E10 and E20 (10 and 20 %vol ethanol, respectively) fuels compared to E0, Knoll *et al.* [13] and Storey *et al.* [14] presented similar observations of significant statistical increases in acetaldehyde emissions between E20 and E10 and E10 and E0, but they also reported no significant change of formaldehyde emissions beyond 10 %vol ethanol addition. De Melo *et al.* [15] tested E25 fuel in a flex-fuel engine and found an increase in the aldehyde and unburned ethanol emissions with ethanol addition. Jin *et al.* [16] explored ethanol blending ratios of 30 - 85 %vol in gasoline and reported ethanol and acetaldehyde emissions were over 5.5 and 300 times higher for the E85 than E0 fuel. Clairotte *et al.* [17] and Suarez-Bertoa *et al.* [18] tested E75 and E85 (with 75 and 85 %vol, respectively) fuels at inlet temperatures of 22 °C and -7 °C and found that acetaldehyde emissions were enhanced at the low temperature condition in comparison to formaldehyde, suggesting different formation mechanisms. Sandstroem-Dahl *et al.* [19] and Gierczak *et al.* [20] also tested E85 fuels and found that aldehyde emissions measurements from the Fourier Transform Infrared (FTIR) spectroscopy gas analyser matched the emissions sampled with 2,4-dinitrophenyl hydrazine (2,4-DNPH) cartridges, the standardised method approved in the USA, and with Flame Ionisation Detector (FID), following EU regulations, respectively. These trends are attributed to the ethanol presence due to the hydroxyl ($-$OH) moiety in alcohol fuels [7]. Ethanol favours OH radical scavenging pathways in comparison to conventional low-temperature chain branching pathways [6, 21]. Ethanol consumption is initiated by hydrogen atom abstraction followed by a β-scission, resulting primarily in acetaldehyde as a stable intermediate. The reaction pathways of ethylhydroxy and α-hydroxyethyl radicals, formed from ethanol's hydrogen atom abstraction, to formaldehyde and acetaldehyde are shown in Reactions 1 and 2, respectively [22].

$$CH_3CH_2O^{\bullet} \iff CH_2O + CH_3^{\bullet} \quad \text{(R1)}$$

$$CH_3C^{\bullet}H_2O \iff CH_3CHO + H^{\bullet} \quad \text{(R2)}$$

Nevertheless, the interactions of ethanol with gasoline components and the contribution of these components to the aldehyde emissions have been minimally studied. Considering a fundamental gasoline representative component, iso-octane, Curran *et al.* suggest that the low temperature oxidation of iso-octane produces large alkoxy radicals [23]. They undergo β-scission to generate stable aldehydes, primarily formaldehyde, a hydrogen atom, and an alkyl radical [23]. In addition, Broustail *et al.* report that for iso-octane, the other pathway to produce formaldehyde is via acetaldehyde [24].

The addition of ethanol to gasoline is associated with a reduction in the aromatic content of the fuels due to both ethanol and aromatic components' high octane characteristics. They are a substitute for each other in the blending process to achieve a target octane rating [25]. Karavalakis *et al.* [26] investigated the effects of increasing aromatic content from 15 to 35 % whilst maintaining all other properties of an E10 market fuel on five gasoline direct injection (GDI) vehicles and found that the changes in fuel composition had no statistically significant effect on the formaldehyde and acetaldehyde emissions. Whereas, Goodfellow *et al.* [27] and Zervas *et al.* [28] found that the lower carbon number aldehydes (formaldehyde and acetaldehyde) decreased with increasing aromatic content. However, Shuetzle *et al.* [29], Yang *et al.* [9], and Zhang et al. [30] found significant impacts of aromatic contents on aldehyde emissions. They suggest that formaldehyde and acetaldehyde are mostly generated by the methyl and ethyl radicals from the partial combustion of iso-paraffins and alkyl aromatics. Another route of acetaldehyde formation is through the decomposition of benzaldehyde which is an inherent intermediate formed during toluene's oxidation [31, 32]. For example, Reaction 3 shows the benzyl radical, produced via toluene's hydrogen abstraction, reacting with atomic oxygen to yield the phenyl radical and formaldehyde. Zhang *et al.* also found that C8 and C9 aromatics strongly favoured aldehyde formation [30]. The different outcomes from these studies highlight the importance to understand the implications of aromatic content and its interactions with other gasoline fuel components on the formation of aldehyde emissions.

$$C_6H_5C^{\bullet}H_2 + O \iff C_6H_5^{\bullet} + CH_2O \qquad \text{(R3)}$$

Beyond aldehyde emissions, Karavalakis *et al.* [26] and Zhu *et al.* [33] reported that non-methane hydrocarbon (NMHC) emissions were decreased with increased aromatic content on GDI vehicles. Schifter *et al.* [34] observed similar behaviour from four port-fuel injection (PFI) vehicles. They attributed the causes to a delay in the light-off of the three-way catalytic (TWC) converter because of lower peak flame temperatures [30]. Whereas Broustail *et al.* [24] found increasing ethanol concentration decreased the total hydrocarbon (THC) emissions component, which includes the NMHC emissions.

Many of these studies are conducted in full vehicle operations where there are many external factors affecting the results. Often, these tests study the emissions after the TWC, which alters the composition of the exhaust based on its temperature amongst other factors. To truly understand the fuel impact, engine-out emissions from a simple engine would be preferable. Therefore, this study explores the impact of ethanol, toluene, and iso-octane, as pure components, as binary mixtures of ethanol and toluene, and as ternary mixtures with varying toluene content on engine-out aldehyde, ethanol, and NMHC emissions. The fuel effects on engine-out aldehyde and NMHC emissions were analysed across varying fuel-to-air equivalence ratio (ϕ), load (measured through the indicated mean effective pressure (IMEP)), and at a constant engine speed of 1100 rpm. The results for the investigated research fuels are presented for the first time in literature to aid the understanding of fuel interactions and engine operating conditions on engine-out emissions.

EXPERIMENTAL SETUP

A single-cylinder, GDI-SI engine with optical access capabilities was used for these experiments. Its configuration is shown in Figure 1. However, none of the optical access characteristics were used for this work. The engine was coupled with a Control Techniques dynamometer for torque and speed control. The test cell was controlled by the Taylor DynPro2 system. The combustion system consisted of a centrally mounted spark plug and the fuel injector was operating at a pressure of 150 bar. The Berkeley Nucleonics Corporation (BNC) model 725 unit controlled injection and ignition timing and injection duration with shaft encoder trigger signals. The engine coolant was maintained at 45 °C to minimise the risk of melting the piston rings. These rings were made of polyamide-imide to achieve oil-free combustion; enabling the effect of the individual fuel components tested here to be studied in isolation. All temperatures were measured with K-type thermocouples. The experimental test facility has previously been comprehensively described by White *et al.* [35].

The Taylor DynPro2 system also logged low-speed data such as the exhaust temperature at 1 Hz. A Kistler Type 6041A high-speed pressure transducer was used to measure the cylinder pressure data. This was recorded at 0.1 °CA resolution using the AVL X-ion high-speed data acquisition system. The indicated mean effective pressure was calculated using the cylinder pressure. High-speed data was collected for 300 cycles once the engine reached stable operation and three independent runs were conducted at each operating point. The fuel-air equivalence ratio (ϕ) was measured using a lambda sensor at the exhaust of the engine. The sensor was calibrated with free air according to the fuel-air ratio of each fuel. The engine specifications and settings are presented in Table 1.

Table 1: Engine specifications and settings.

Parameter	Unit	Value
Bore	mm	89.0
Stroke	mm	90.3
Displacement	cm^3	561.9
Compression ratio	-	11:1
Fuel pressure	bar	150
Valves per cylinder	-	2 intake; 2 exhaust
IVO	°CA aTDC	-336
IVC	°CA aTDC	-86
EVO	°CA aTDC	116
EVC	°CA aTDC	366
Injection timing	°CA aTDC	-270
Ignition timing	°CA aTDC	-46.3

A Fourier transform infrared spectroscopy (FTIR) gas analyser (AVL SESAM FTIR i-60) was used to measure real-time engine-out emissions. The FTIR analyser operates at a sampling rate of 5 Hz. With a gas cell capacity of 200 mL, the FTIR analyser operates with a sample flow rate of 8 L/min maintaining 191 °C and 800 hPa to achieve effective gas exchange at this rate. Prior to each fuel test, the background spectrum used to determine absorbance was collected and normalised by purging the gas cell with nitrogen gas. Through operating at 191 °C, the FTIR analyser samples the raw exhaust without contaminating the optics with water vapour and emission constituents. Upstream, the FTIR analyser sample line is also heated to 191 °C thus preventing losses from adsorption and condensation. Between the engine-out exhaust and the heated line, a heated filter removes particulate matter to prevent optical cell contamination. This filter was replaced with a new one for each fuel tested. The specifications of the relevant measured emissions can be found in Table 2. For the non-methane hydrocarbon (NMHC) emissions, the FTIR identifies a group of hydrocarbons (HCs), including oxy-

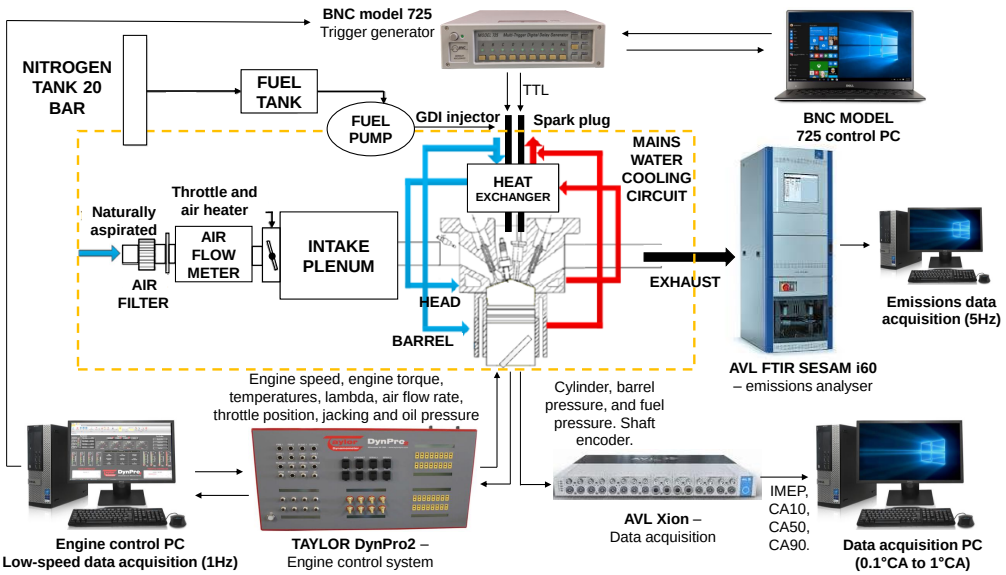

Figure 1: Single cylinder engine configuration

genated species and excluding methane, that are present in the exhaust above pre-determined threshold levels. The analysis of infrared spectra works best for HCs with low carbon numbers as they have strong and sharp absorbance bands [36]. As the top ten compounds account for 80% of the HCs in the exhaust, Gierczak *et al.* [20] found that the FTIR method yielded FTIR equivalent NMHC measurements within 5% of the regulatory flame ionisation detection (FID) method for fuel blends ranging from gasoline to E85 (85 %vol ethanol and 15 %vol gasoline).

Table 2: FTIR emissions analyser specifications for emissions considered in this paper.

Emission component	Name	Unit	Range	Accuracy
Formaldehyde	HCHO	ppm	0-1000	± 0.15
Acetaldehyde	MECHO	ppm	0 - 3000	± 0.35
Ethanol	ETOH	ppm	0 - 1000	± 0.30
Non-methane hydrocarbons	NMHC	ppm	0 - 10000	± 2.50

EXPERIMENTAL METHODOLOGY

The engine was first warmed up with the coolant temperatures stabilised. All the tests were carried out at ambient air intake conditions (298 ± 5 K), at an engine speed of 1100 rpm. The fuel-air equivalence ratio (ϕ) and IMEP were controlled by adjusting the throttle position and injection duration. For each test, the data from 300 consecutive cycles were measured and then averaged. Three runs were performed for each operating condition. The effect of toluene, ethanol, and iso-octane (2,2,4-trimethylpentane), and their binary and ternary mixtures on engine-out emissions was studied. The molar and volumetric compositions of the eight fuels tested are shown in Table 3.

The iso-octane, toluene, and ethanol were all sourced from Thermo Fischer Scientific and had 99.8%, 99.9%, and 99.5% purity, respectively, as stated by the supplier. Through testing bespoke binary and ternary mixtures, the precise effects of the interactions between ethanol, toluene, and iso-octane (common gasoline surrogate components) on engine-out emissions can be quantified and studied. The conditions tested and the range is shown in Table 4.

Table 3: The volumetric and molar fractions of the fuels tested.

Fuel	Ethanol		Toluene		Iso-octane	
	mol	vol	mol	vol	mol	vol
E100	1.00	1.00	-	-	-	-
O100	-	-	-	-	1.00	1.00
T100	-	-	1.00	1.00	-	-
TE25	0.38	0.25	0.62	0.75	-	-
TE50	0.65	0.50	0.35	0.50	-	-
TE75	0.85	0.75	0.15	0.25	-	-
OTE25_LowT	0.48	0.25	0.05	0.05	0.47	0.70
OTE25_HighT	0.44	0.25	0.29	0.35	0.28	0.40

Table 4: The operating conditions investigated.

Condition	Equivalence ratio (ϕ)	Speed	IMEP
value	0.90 - 1.20	1100	1.8 - 3.00
range (±)	0.02	10	0.25

For each fuel and operating condition, the measured cylinder pressure profiles were averaged over 300 consecutive cycles and 3 repeats. The cylinder temperature profiles were derived from the pressure traces. These data are presented in Appendix A.

For each dataset, the emissions skewed by anomalous peaks detected by the FTIR analyser due to partial burns or misfires were excluded. Across all tests, the median coefficient of variation (CoV) of IMEP was 4 %.

The results presented are an average of three independent runs collected for 300 consecutive cycles each. The error bars on the results plots represent the maximum and minimum of the respective emission from each run.

RESULTS AND DISCUSSION

The results are reported in three sections: the effect of each fuel tested on engine-out aldehyde emissions at stoichiometric low load and speed conditions; the impact of varying the fuel-air equivalence ratio for each of the fuels studied; and the influence of increased IMEP for the ternary mixtures.

EFFECT OF FUEL COMPOSITION

The engine-out emissions of pure fuel constituents ethanol, toluene, and iso-octane, binary mixtures of ethanol and toluene with increasing ethanol ratio, and ternary mixtures of iso-octane and ethanol with low and high levels of toluene, defined by the EN228 standards' limit [37]. Through understanding the behaviour of the components individually, their contribution to engine-out aldehyde emissions in specifically curated binary and ternary mixtures can be investigated.

Pure fuels

At 1.80 bar IMEP / 1100 rpm, stoichiometric conditions, the engine-out formaldehyde and acetaldehyde emissions are compared for ethanol, toluene, and iso-octane as shown in Figure 2. Figure 2 shows that ethanol gives greater formaldehyde and acetaldehyde emissions than both toluene and iso-octane. A ten- and five-fold increase in average engine-out aldehyde emissions was produced from ethanol compared to toluene and iso-octane, respectively. This agrees with literature that identifies that aldehyde engine-out emissions for pure ethanol combustion are significantly greater than conventional gasoline fuel with components including iso-octane and toluene [38]. Nevertheless, to the author's knowledge, this is the first time in the open literature that the engine-out aldehyde emissions of iso-octane and toluene are presented in comparison to pure ethanol.

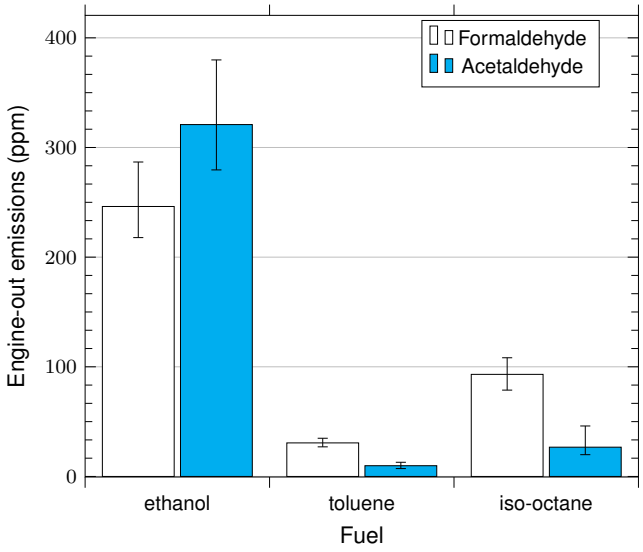

Figure 2: Formaldehyde (white) and acetaldehyde (cyan) engine-out emissions for ethanol, toluene, and iso-octane at 1.80 bar IMEP / 1100 rpm, stoichiometric conditions. Error bars represent minimum and maximum emissions over three runs.

Furthermore, Figure 2 shows that the formaldehyde to acetaldehyde ratio for ethanol is approximately 0.76 for ethanol, however, for toluene and iso-octane, this ratio is around 3.0. The observed increased formation of acetaldehyde over formaldehyde for ethanol agrees with the literature as the fundamental combustion chemistry of ethanol as previously described by Reactions 1 and 2 [7, 22]. Whereas, for iso-octane, these findings agree with the work of Curran *et al.* [23] and Broustail *et al.* [24] which report iso-octane's reaction pathways lead to greater formaldehyde than acetaldehyde emissions. Similarly, for toluene, whilst the measured acetaldehyde emissions are negligible compared to ethanol, the formaldehyde emissions can be attributed to Reaction 3. Furthermore, this indication of greater formaldehyde than acetaldehyde for conventional gasoline components with no ethanol is in line with literature as Wang *et al.* [38] found similar results with unleaded gasoline from a single-cylinder engine.

By investigating pure fuel constituents of gasoline, the engine-out aldehyde emissions were measured in real-time and presented from a direction injection SI engine. These results clearly show that the direct impact of the combustion of toluene produces significantly less engine-out aldehyde emissions than ethanol and iso-octane, a simple gasoline surrogate. As toluene has a higher adiabatic flame temperature, this could also be attributed to the higher in-cylinder combustion temperatures which consume the aldehydes. To further understand the impact of aromatic components in aldehyde engine-out emissions, binary blends of toluene and ethanol were studied.

Binary mixtures

At similar operating conditions to the pure fuels, with 1.80 bar IMEP / 1100 rpm, stoichiometric conditions, three binary fuels were investigated. Figure 3 presents the formaldehyde and acetaldehyde emissions. The results indicate that for TE25, the acetaldehyde and formaldehyde emissions are at similar levels and hence the formaldehyde to acetaldehyde ratio is 1.20, whereas, with increasing ethanol addition, the ratio changes to approximately 0.70, showing greater acetaldehyde than formaldehyde emissions. Furthermore, the difference between formaldehyde and acetaldehyde emissions increases with ethanol addition. Since ethanol is one of the main precursors of aldehyde emissions, these trends are expected and in line with the results seen from the pure component fuels.

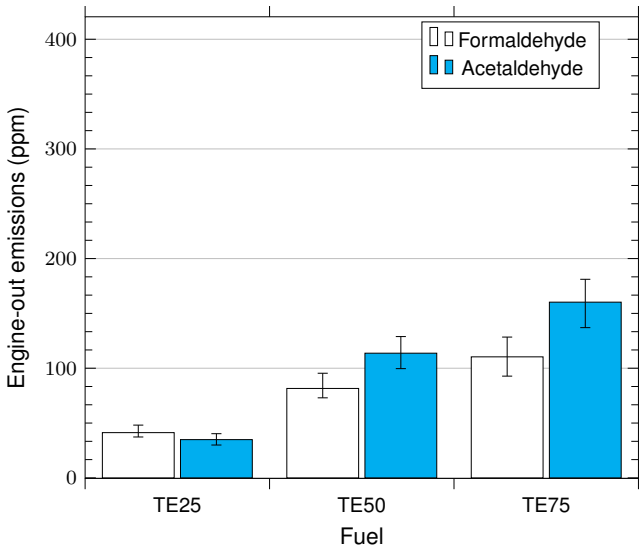

Figure 3: Formaldehyde (white) and acetaldehyde (cyan) engine-out emissions for TE25, TE50, and TE75 at 1.80 bar IMEP / 1100 rpm, stoichiometric conditions. Error bars represent minimum and maximum emissions over three runs.

When comparing the binary mixture with its pure fuel constituents of ethanol and toluene, Figure 4 shows that even with 25 %vol addition of toluene to a binary TE mixture, the aldehyde emissions are halved compared to pure ethanol. This could be attributed to toluene's presence increasing the in-cylinder temperature or leading to pockets of high temperature in the cylinder consuming the intermediate aldehydes.

These findings, albeit from fuel compositions that are not typically expected in an engine, aid the understanding of the interactions of aromatic and oxygenate fuel components and their implication on aldehyde engine-out emissions. When studying ignition delay time and flame speed, Fan *et al.* [39] reported that the increased $HO_2^{\bullet}$ radical production from ethanol led to faster consumption of the benzyl radical from toluene. Specif-

ically, during the low temperature heat release, the reactivity of ethanol is suppressed but the reactivity of toluene is significantly enhanced [39]. Similar observations have been made when studying the laminar burning velocity of equal-volume binary and ternary mixtures of iso-octane, ethanol, and toluene at 380 K and 450 K [40, 41, 42]. As Sarathy *et al.* found, in this region, ethanol favours chain termination pathways leading to acetaldehyde [7]. However, as these reactions are suppressed by toluene's increased reactivity, the measured engine-out aldehyde emissions are significantly reduced.

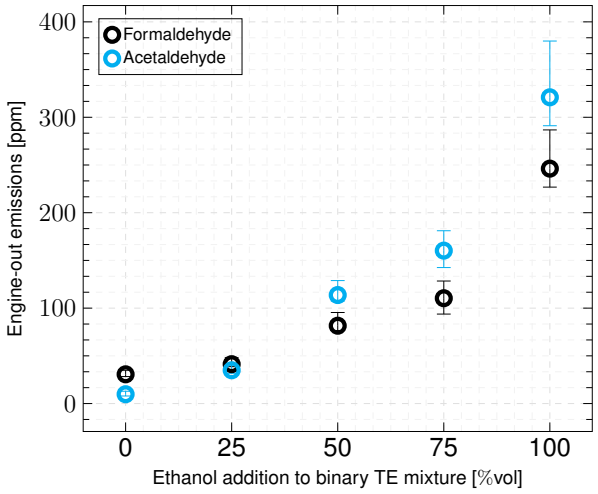

Figure 4: Binary fuel mixtures formaldehyde, acetaldehyde, and ethanol engine-out emissions at 1.8 bar IMEP / 1100 rpm, stoichiometric conditions. Error bars represent minimum and maximum emissions per run.

These results show that toluene exhibits a suppressing effect on the engine-out aldehyde emissions of pure ethanol. To explore toluene's influence on other common gasoline surrogate components, the effect of low and high concentrations on a simple E25 (25 and 75 %vol of ethanol and iso-octane, respectively) gasoline surrogate is studied.

Ternary mixtures

Similar to the pure and binary fuels, the ternary mixtures were investigated at an IMEP of 1.95 bar IMEP / 1100 rpm, stoichiometric conditions. Figure 5 presents the formaldehyde, acetaldehyde, and ethanol engine-out emissions from the two ternary mixtures.
Figure 5 show that on average, the aldehyde emissions from the OTE25_LowT ternary mixture are higher than OTE25_HighT. As the latter composition has less iso-octane, a precursor to formaldehyde, this could lead to lower aldehyde emissions on average. As seen with the binary mixtures, the increased toluene presence in OTE25_HighT can suppress the reactivity of ethanol, thus lowering the aldehyde emissions.

Furthermore, the ternary mixtures' formaldehyde to acetaldehyde ratio is approximately 2.0, which is lower than the ratio of 3.0 found for pure iso-octane and toluene. This is directly related to the presence of ethanol in the blends, highlighting that the acetaldehyde concentration has increased despite the suppression of ethanol's reactivity.

Figure 5 also shows the engine-out unburned ethanol emissions. For both ternary mixtures, the ethanol emissions are similar at approximately 105 ppm. As an single-cylinder engine with optical access capabilities was used for these experiments, the unburned ethanol in part comes from the combustion chamber crevices, which are large compared to production engines. However, at the same operating conditions, pure ethanol combustion led to an average of 1490 ppm of ethanol emissions, which represents a 14-fold increase. This could illustrate the chemical ki-

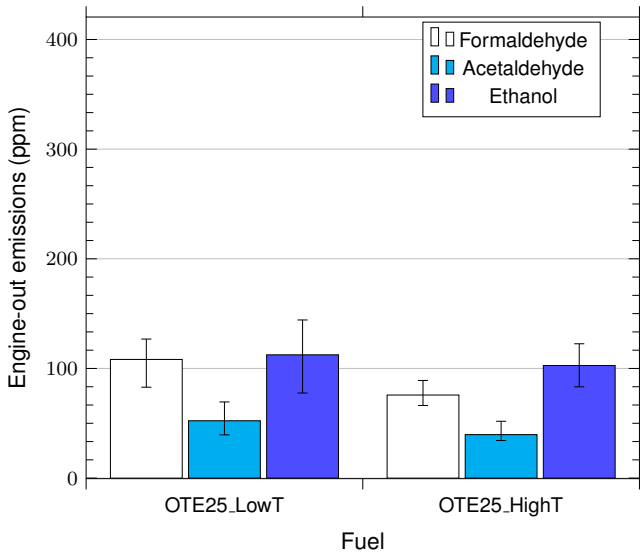

Figure 5: Formaldehyde (white), acetaldehyde (cyan), and ethanol (blue) engine-out emissions for OTE25_LowT and OTE25_HighT at 1.95 bar IMEP / 1100 rpm, stoichiometric conditions. Error bars represent minimum and maximum emissions over three runs.

netic effect of toluene in the fuel composition and suggests that the increased toluene presence leads to local areas of high temperature within the combustion chamber that partially consumes the ethanol, resultant aldehydes, and other intermediates from ethanol combustion.

Furthermore, to understand iso-octane's impact, the unburned ethanol emissions between TE25 and the ternary mixtures can be compared (as iso-octane's presence at varying quantities is their main difference). TE25's combustion leads to around 165 ppm of unburned ethanol emissions at the aforementioned conditions. This suggests iso-octane's low-temperature reactivity could promote the consumption of ethanol, however, this effect is predicted to be lower than that of toluene.

Summary

The results illustrate that compared to iso-octane and ethanol, toluene as a pure component produces minimal formaldehyde and acetaldehyde engine-out emissions. When toluene is mixed with ethanol, the increased reactivity of toluene, partially due to the HO_2 radicals production from ethanol [39], suppresses the engine-out aldehyde emissions of the mixture. For ternary mixtures of iso-octane, toluene, and equivalent volumetric concentration of ethanol, the increased presence of toluene leads to lower engine-out aldehyde emissions. The results agree with Goodfellow *et al.* [27] and Zervas *et al.* [28] that lower carbon number aldehydes decreased with increasing aromatic content. Whereas, the results from this work differ from the findings of Yang *et al.* [9], Schuetzle *et al.* [29], and Zhang *et al.* [30] where formaldehyde and acetaldehyde formation was linked to aromatic content. These experiments were conducted on a vehicle level with three-way catalysts (TWC). This would likely alter the composition of the exhaust gases based on operating conditions and TWC temperatures.

EFFECT OF FUEL-AIR EQUIVALENCE RATIO

During transient conditions in a normally operating engine, there are points at which rich (excess fuel) or lean (excess air) conditions are briefly encountered in the engine. This section explores the impact of equivalence ratio on aldehyde engine-out emissions at 1.80 bar IMEP / 1100 rpm.

Pure fuels

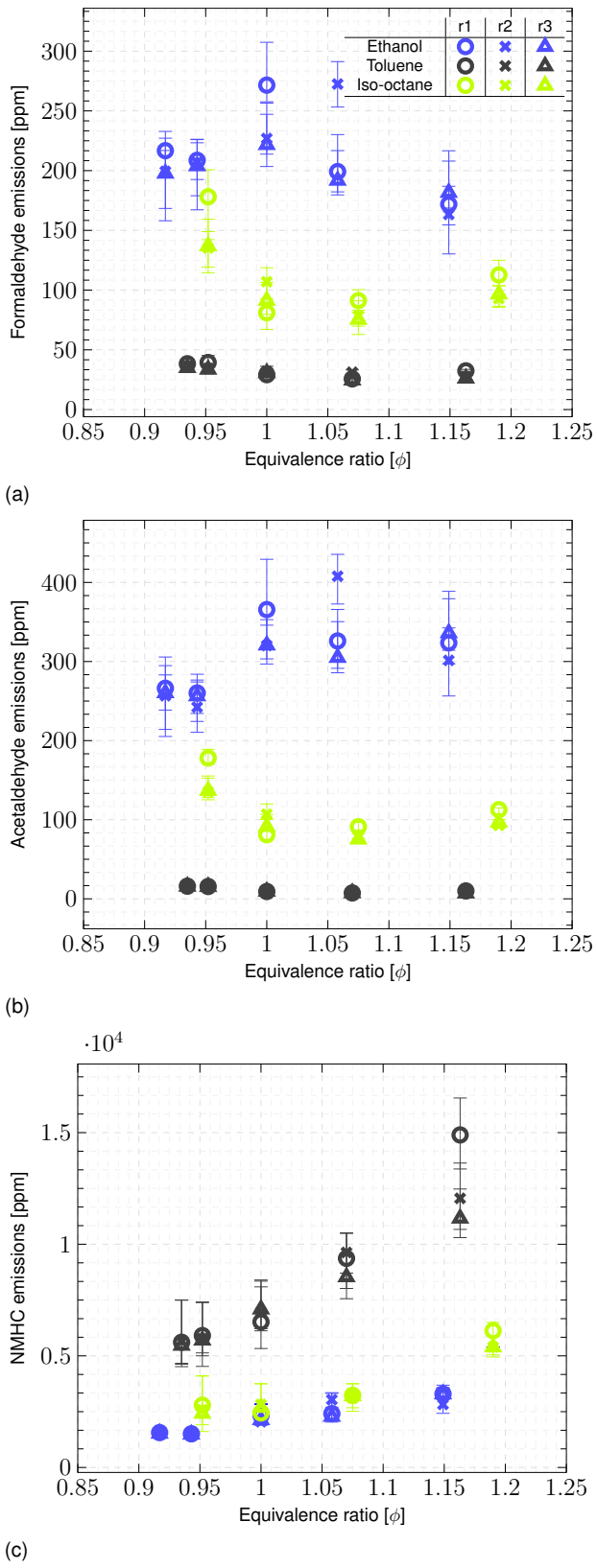

Figure 6: Ethanol (blue), toluene (black), and iso-octane (green) engine-out a) formaldehyde, b) acetaldehyde, and c) NMHC emissions across an equivalence ratio (ϕ) range at 1.80 bar IMEP, 1100 rpm. Error bars represent minimum and maximum emissions per run.

The formaldehyde, acetaldehyde, and non-methane hydrocarbons (NMHC) engine-out emissions from the pure fuels of ethanol (blue), toluene (black), and iso-octane (green) are presented in Figure 6. At each of the fuel-air equivalence ratios (ϕ) tested, ethanol presents greater engine-out aldehyde emissions than iso-octane and toluene similar to the distinction across the three fuels at stoichiometric conditions. For the combustion of pure ethanol, the formaldehyde and acetaldehyde engine-out emissions peak at stoichiometric ($\phi = 1$), however, they decrease at lean ($\phi < 1$) and rich ($\phi > 1$) conditions. Zervas *et al.* present similar findings when they tested fuels with ethanol blended [28]. Due to the inherent oxygen content in ethanol compared to the other fuels tested, the additional oxygen content leads to the oxidation and consumption of the intermediate aldehydes at the richer conditions. At the lean operating conditions, ethanol's greater propagating flame speed is favoured by the retarded ignition timing as it is fixed across all tests and additional oxygen content as similarly observed by Yu *et al.* [43]

However, for iso-octane and toluene, a relative increase in the engine-out aldehyde emissions is observed at the lean operating condition. Compared to ethanol, both these components have slower flame speeds as identified by Dirrenberger *et al.* [44]. As the ignition timing is fixed and potentially too retarded for iso-octane and toluene, there is a greater amount of unburned intermediates at the lean operating condition. This suggests an advanced ignition time would lead to lower aldehyde emissions at this condition.

The increased aldehyde emissions at lean conditions are particularly observed with iso-octane, which is more susceptible to pre-spark ignition than toluene. Furthermore, compared to both toluene and ethanol, iso-octane represents two-stage reactivity [45]. This could also lead to an increased quantity of unburned intermediate aldehydes.

For the pure fuels tested, the opposite trend to aldehydes is observed for NMHC. Ethanol emits the lowest concentration of NMHC, whereas toluene emits the highest among the fuels tested across the range of equivalence ratios. As the mixture becomes leaner, the NMHC clearly presents decreasing trends, whereas, toluene and iso-octane lead to increased aldehyde emissions at lean conditions. This could be due to the aldehydes formed as stable intermediates and not due to partial or incomplete combustion. The interactions and resultant emissions of these fuels in binary compositions across the equivalence ratio range were also studied.

Binary mixtures

The formaldehyde, acetaldehyde, and NMHC engine-out emissions from the binary mixtures of TE25 (orange), TE50 (magenta), and TE75 (teal) are presented in Figure 7.

For the three binary toluene and ethanol (TE) mixtures tested, a difference in formaldehyde and acetaldehyde emissions between the fuels is observed across the equivalence ratio range. The mixture with the greatest content of ethanol (TE75) produces two to three times more engine-out aldehyde emissions compared to the mixture with the least (TE25). The rate of increase in engine-out aldehyde emissions is greater between TE75 and TE50 than between TE50 and TE25. This further affirms that ethanol is a major precursor to aldehyde formation. However, the presence of toluene suppresses ethanol's oxidation to aldehydes as previously described at stoichiometric conditions. This is effective when the majority of the binary composition is toluene (i.e., TE50 and TE25).

In contrast to pure ethanol's behaviour at rich conditions where the aldehyde emissions decrease, for all binary mixtures tested, the aldehyde emissions increased at these conditions. This could be attributed to the additional oxygen in ethanol consumed by toluene as it has enhanced reactivity when coupled with

ethanol.

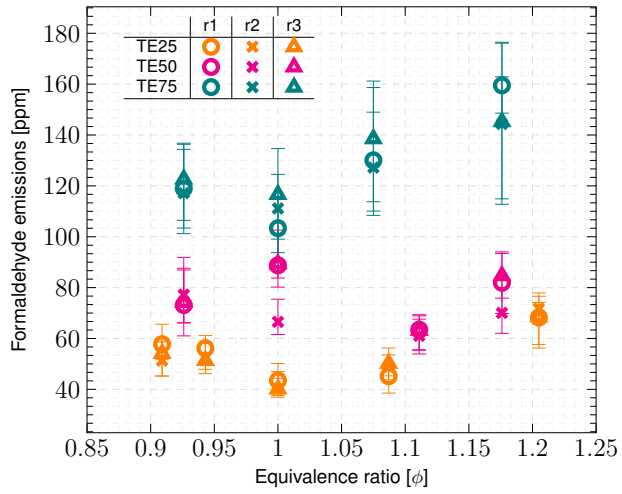

(a)

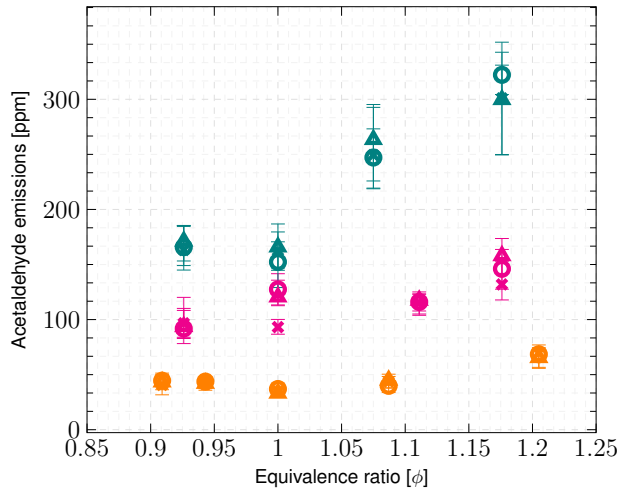

(b)

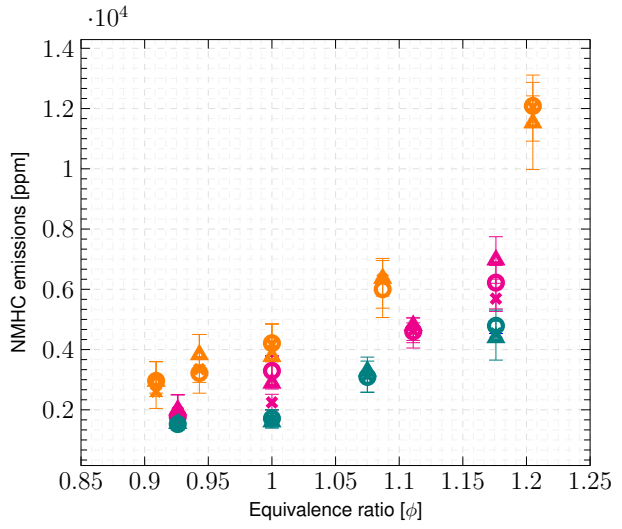

(c)

Figure 7: TE25 (orange), TE50 (magenta), and TE75 (teal) fuels with engine-out a) formaldehyde, b) acetaldehyde, and c) NMHC emissions across an equivalence ratio (ϕ) range at 1.80 bar IMEP / 1100 rpm. Error bars represent minimum and maximum emissions per run.

The NMHC engine-out emissions were greatest for the TE25 mixture, which has the highest toluene concentration, and lowest for the TE75 mixture. The opposite behaviour was observed for aldehyde emissions. However, based on the findings of the pure components, this trend is expected. The interactions between toluene and ethanol present insightful results on their complementary role to each other. Ethanol enables the reduction of toluene's NMHC emissions due to its fuel-bound oxygen and toluene reduces the aldehyde emissions of ethanol by suppressing its formation reactions. The impact of these interactions with a simple gasoline surrogate of iso-octane was studied across the same equivalence ratio range.

Ternary mixtures

Similar to the pure fuels and binary mixtures, the ternary mixtures of OTE25_LowT (brown) and OTE25_HighT (violet) were tested at 1.9 bar IMEP, 1100 rpm, across an equivalence ratio (ϕ) range of 0.90 to 1.20. The formaldehyde, acetaldehyde, and NMHC engine-out emissions are presented in Figure 8. Over the equivalence ratios tested, the engine-out aldehyde emissions for the OTE25_LowT ternary mixture were greater than the OTE25_HighT. Despite consistent levels of ethanol in both fuels, the displacement of iso-octane in the OTE25_LowT fuel led to reduced aldehyde emissions. This follows observations made for the pure constituents of these mixtures where iso-octane produces twice the amount of aldehyde emissions as toluene.

At the richer conditions ($\phi > 1$), the difference in formaldehyde emissions between the fuels is greater, however, for acetaldehyde and NMHC, this difference is less obvious. As iso-octane presents a formaldehyde-to-acetaldehyde ratio of 3:1, its presence at a greater concentration for the OTE25_LowT mixture could explain the clear difference in formaldehyde emissions. From rich to stoichiometric operating conditions, a reduction in engine-out emissions is observed, as expected. However, beyond stoichiometric, at lean conditions, the average engine-out emissions are greater than at stoichiometric. Due to the low flame propagating speeds of iso-octane and toluene, this could be attributed to the fixed ignition timing which may be too retarded for these pure fuel constituents which form a major part of the ternary mixture. Similar behaviour was observed for pure iso-octane and toluene.

Although there is a greater toluene concentration in OTE25_HighT, at rich conditions, the mixture's NMHC engine-out emissions are lower than OTE25_LowT. At stoichiometric, the NMHC emissions are comparable for both fuels and at leaner conditions, a shift in trend where OTE25_HighT has greater NMHC emissions is observed, albeit within the error range of OTE25_LowT.

For both mixtures, at the rich conditions, the spread in emissions measurements is greater. Furthermore, the error bars for OTE25_LowT are greater than OTE25_HighT suggesting that the increased presence of toluene has led to more predictable and stable emissions.

These results indicate that the aldehyde engine-out emissions are increased with mixtures that contain a lower concentration of aromatics, represented by toluene in this work, at low speed and load conditions. Whilst the difference is minimal at stoichiometric, the discrepancies disproportionately increase at rich operating conditions. To explore whether this behaviour is replicated at partially higher loads, the ternary mixtures were tested at 3.0 bar IMEP and 1100 rpm.

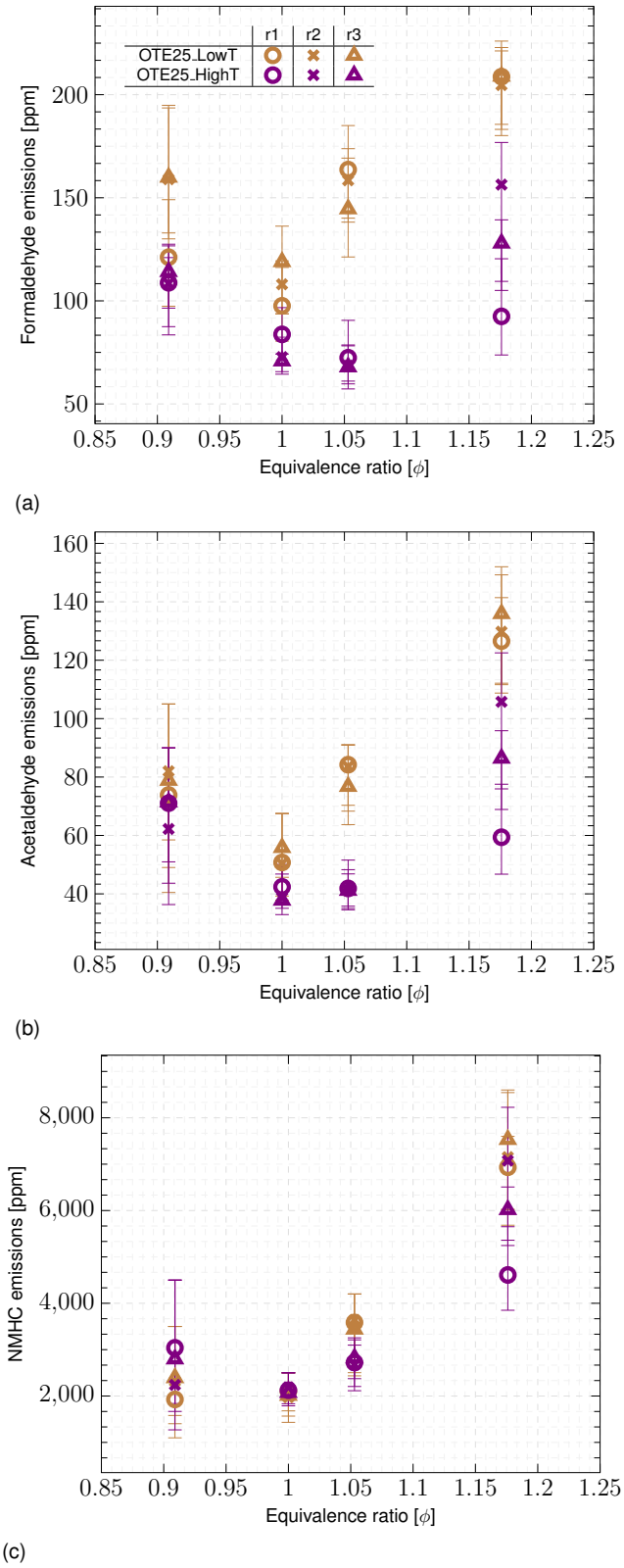

Figure 8: OTE25_LowT (brown) and OTE25_HighT (violet) fuels with engine-out a) formaldehyde, b) acetaldehyde, and c) NMHC emissions across an equivalence ratio (ϕ) range at 1.95 bar IMEP / 1100 rpm. Error bars represent minimum and maximum emissions per run.

EFFECT OF LOAD

Figure 9 presents the formaldehyde, acetaldehyde, and NMHC engine-out emissions from the OTE25_LowT and OTE25_HighT at 1.95 and 3.00 bar IMEP, 1100 rpm, and stoichiometric conditions.

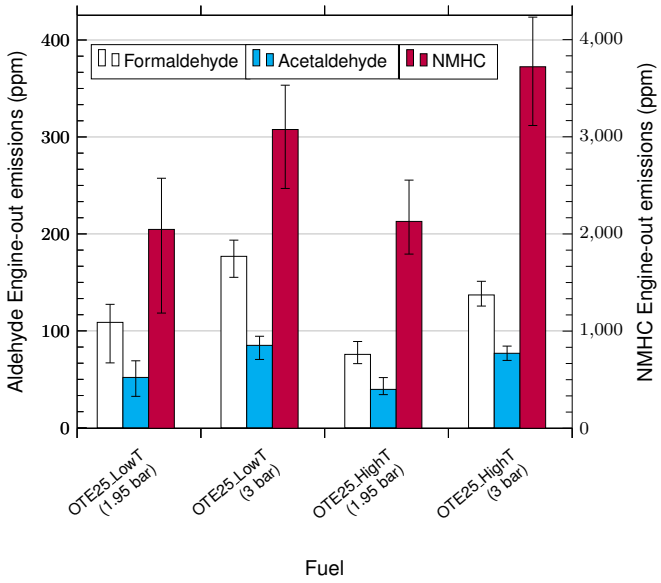

Figure 9: Formaldehyde (white), acetaldehyde (cyan), and NMHC (red) engine-out emissions for OTE25_LowT and OTE25_HighT at IMEPs of 1.95 and 3.00 bar / 1100 rpm, stoichiometric conditions. Error bars represent minimum and maximum emissions over three runs.

As the load increases, the resultant engine-out emissions increase. This can be attributed to the increased fuelling at a higher load. For both fuels, the injected quantity increased by approximately 33 %. Furthermore, the OTE25_LowT presents greater engine-out aldehyde emissions than OTE25_HighT at the higher load operating point following the trend previously observed. However, the rate of increase in engine-out aldehyde and NMHC emissions is greater for OTE25_HighT than OTE25_LowT. This shows that low-speed conditions present unfavourable combustion conditions for toluene, thus accelerating the rate of increase in emissions for the higher toluene concentration ternary mixture.

For both operating loads and fuels, the formaldehyde-to-acetaldehyde ratio is approximately 2:1. Whilst this ratio is moderately higher than 2:1 for OTE25_LowT, the opposite is observed for OTE25_HighT. Following the observations made with the binary TE mixtures, the increased presence of toluene in the latter mixture may inhibit ethanol's formation of aldehyde emissions.

A clear distinction in the NMHC engine-out emissions is observed between the two ternary mixtures at the 3 bar load operating condition, whilst they were comparable at a load of 2 bar. This can be attributed to the increased fuel injection but low combustion pressures and temperatures. The results further affirm that these conditions are not optimised for the inherent combustion properties of toluene and iso-octane, leading them to not completely combust. These observations can also explain the increased aldehyde emissions whose production is favoured by the low temperature conditions.

These results also showed that at low speed and load operating conditions, the presence of toluene in an ethanol-gasoline surrogate mixture would inhibit ethanol's formation of aldehyde engine-out emissions.

CONCLUSION

This work explores the engine-out formaldehyde, acetaldehyde, ethanol, and NMHC emissions from eight different fuels. These include pure fuels of ethanol, toluene, and iso-octane, binary mixtures of ethanol and toluene with increasing ethanol ratios (TE25, TE50, TE75, respectively), and two ternary mixtures with low and high concentrations of toluene (OTE25_LowT and OTE25_HighT, respectively). All fuels were tested at an IMEP of 1.80 bar, speed of 1100 rpm, and across a fuel-air equivalence ratio (ϕ) range of 0.90 to 1.20. Ternary mixtures were also tested at a higher load of 3.00 bar IMEP at 1100 rpm, stoichiometric conditions. For all the fuels, at each operating condition, 3 independent tests were performed each with 300 consecutive cycles. The error bars for each test represented the maximum and minimum values from the emissions measurement profiles.

The findings from this work include:

- A ten- and five-fold increase in average engine-out aldehyde emissions was produced from ethanol compared to toluene and iso-octane, respectively. These results clearly identify that the combustion chemistry of pure toluene leads to negligible quantities of aldehyde emissions.
- The formaldehyde to acetaldehyde ratio ranged from 1.20 for TE25 to 0.70 for TE75, showing that increasing ethanol addition to toluene led to greater acetaldehyde production.
- Compared to pure ethanol, 25 %vol addition of toluene to form the TE75 binary mixture halved the average engine-out aldehyde emissions. This suggests a significant suppressing effect by toluene on ethanol's aldehyde formation.
- The ternary mixture with a higher concentration of toluene OTE25_HighT produced lower average engine-out aldehyde emissions compared to OTE25_LowT despite both mixtures having equivalent ethanol quantity. This further affirms toluene's suppressing effect and the contribution of iso-octane to formaldehyde emissions.
- Across the equivalence ratio range, ethanol presents lower aldehyde emissions at lean and rich conditions compared to stoichiometric. However, iso-octane and toluene present contrasting results with greater aldehyde emissions at lean and rich conditions than stoichiometric. This could be attributed to the greater flame speed of ethanol favoured by the retarded ignition timing and the additional oxygen in the ethanol enabling more complete combustion.
- Binary and ternary mixtures followed similar trends across the equivalence ratio as iso-octane and toluene. Increasing ethanol content in the binary mixtures increased the aldehyde emissions. Increased toluene in ternary mixtures reduced the aldehyde emissions across the equivalence ratio range.
- The NMHC emissions reveal that toluene and iso-octane did not completely combust due to their inherent combustion properties thus leading to intermediate aldehyde emissions. Whereas for ethanol, its oxidation process leads to aldehydes directly.

The results from this work indicate that the addition of aromatic content, such as toluene, reduces the aldehyde emission production of ethanol as the benzyl radical consumes the HO_2 radical produced during ethanol's oxidation thus increasing the reactivity of toluene and the in-cylinder temperature. This temperature range provides the environment that consumes the intermediate aldehydes.

References

1. K. Senecal and F. Leach, *Racing toward zero : the untold story of driving green*. 2021.
2. F. Kazemiparkouhi, T. M. Alarcon Falconi, D. L. MacIntosh, and N. Clark, "Comprehensive us database and model for ethanol blend effects on regulated tailpipe emissions," *Science of The Total Environment*, vol. 812, p. 151426, 2022.
3. "Renewable energy directive," *Official Journal of the European Union*, vol. 52, 2009.
4. "Ethanol blending in india 2020-25 roadmap for report of the expert committee," 2021.
5. R. Singh, A. Shukla, S. Tiwari, and M. Srivastava, "A review on delignification of lignocellulosic biomass for enhancement of ethanol production potential," *Renewable and Sustainable Energy Reviews*, vol. 32, pp. 713–728, 2014.
6. S. Cheng, D. Kang, A. Fridlyand, S. S. Goldsborough, C. Saggese, S. Wagnon, M. J. McNenly, M. Mehl, W. J. Pitz, and D. Vuilleumier, "Autoignition behavior of gasoline/ethanol blends at engine-relevant conditions," *Combustion and Flame*, vol. 216, pp. 369–384, 2020.
7. S. M. Sarathy, P. Oßwald, N. Hansen, and K. Kohse-Höinghaus, "Alcohol combustion chemistry," *Progress in Energy and Combustion Science*, vol. 44, pp. 40–102, 2014.
8. F. C. Leach, R. Stone, D. Richardson, J. W. Turner, A. Lewis, S. Akehurst, S. Remmert, S. Campbell, and R. Cracknell, "The effect of oxygenate fuels on pn emissions from a highly boosted gdi engine," *Fuel*, vol. 225, pp. 277–286, 2018.
9. J. Yang, P. Roth, T. Durbin, and G. Karavalakis, "Impacts of gasoline aromatic and ethanol levels on the emissions from gdi vehicles: Part 1. influence on regulated and gaseous toxic pollutants," *Fuel*, vol. 252, pp. 799–811, 2019.
10. D. Schuch, E. D. de Freitas, S. I. Espinosa, L. D. Martins, V. S. B. Carvalho, B. F. Ramin, J. S. Silva, J. A. Martins, and M. de Fatima Andrade, "A two decades study on ozone variability and trend over the main urban areas of the são paulo state, brazil," *Environmental Science and Pollution Research*, 2019.
11. IARC, "IARC Monograph: Chemical agents and related occupations. A review of human carcinogens.," *IARC monographs on the evaluation of carcinogenic risks to humans / World Health Organization, International Agency for Research on Cancer*, vol. 100F, no. Pt F, pp. 9–562, 2012.
12. M. Z. Jacobson, "Effects of ethanol (E85) versus gasoline vehicles on cancer and mortality in the United States," *Environmental Science and Technology*, vol. 41, no. 11, pp. 4150–4157, 2007.
13. K. Knoll, B. West, S. Huff, J. Thomas, J. Orban, and C. Cooper, "Effects of mid-level ethanol blends on conventional vehicle emissions," *SAE Technical Papers*, 2009.
14. J. M. Storey, T. Barone, K. Norman, and S. Lewis, "Ethanol blend effects on direct injection spark- ignition gasoline vehicle particulate matter emissions," *SAE International Journal of Fuels and Lubricants*, vol. 3, pp. 650–659, 12 2010.
15. T. C. C. de Melo, G. B. Machado, C. R. Belchior, M. J. Colaço, J. E. Barros, E. J. de Oliveira, and D. G. de Oliveira, "Hydrous ethanol–gasoline blends – combustion and emission investigations on a flex-fuel engine," *Fuel*, vol. 97, pp. 796–804, 2012.
16. D. Jin, K. Choi, C.-L. Myung, Y. Lim, J. Lee, and S. Park, "The impact of various ethanol-gasoline blends on particulates and unregulated gaseous emissions characteristics from a spark ignition direct injection (sidi) passenger vehicle," *Fuel*, vol. 209, pp. 702–712, 2017.
17. M. Clairotte, T. Adam, A. Zardini, U. Manfredi, G. Martini, A. Krasenbrink, A. Vicet, E. Tournié, and C. Astorga, "Ef-

fects of low temperature on the cold start gaseous emissions from light duty vehicles fuelled by ethanol-blended gasoline," *Applied Energy*, vol. 102, pp. 44–54, 2013. Special Issue on Advances in sustainable biofuel production and use - XIX International Symposium on Alcohol Fuels - ISAF.

18. R. Suarez-Bertoa, A. Zardini, H. Keuken, and C. Astorga, "Impact of ethanol containing gasoline blends on emissions from a flex-fuel vehicle tested over the worldwide harmonized light duty test cycle (wltc)," *Fuel*, vol. 143, pp. 173–182, 2015.

19. C. Sandstroem-Dahl, L. Erlandsson, J. Gasste, and M. Lindgren, "Measurement methodologies for hydrocarbons, ethanol and aldehyde emissions from ethanol fuelled vehicles," *SAE Technical Papers*, pp. 453–466, 2010.

20. C. A. Gierczak, L. L. Kralik, A. Mauti, A. L. Harwell, and M. M. Maricq, "Measuring nmhc and nmog emissions from motor vehicles via ftir spectroscopy," *Atmospheric Environment*, vol. 150, pp. 425–433, 2017.

21. F. M. Haas, M. Chaos, and F. L. Dryer, "Low and intermediate temperature oxidation of ethanol and ethanol–prf blends: An experimental and modeling study," *Combustion and Flame*, vol. 156, no. 12, pp. 2346–2350, 2009.

22. G. da Silva, J. W. Bozzelli, L. Liang, and J. T. Farrell, "Ethanol oxidation: Kinetics of the α-hydroxyethyl radical + o2 reaction," *The Journal of Physical Chemistry A*, vol. 113, no. 31, pp. 8923–8933, 2009. PMID: 19594149.

23. H. Curran, P. Gaffuri, W. Pitz, and C. Westbrook, "A comprehensive modeling study of iso-octane oxidation," *Combustion and Flame*, vol. 129, no. 3, pp. 253–280, 2002.

24. G. Broustail, F. Halter, P. Seers, G. Moréac, and C. Mounaim-Rousselle, "Comparison of regulated and non-regulated pollutants with iso-octane/butanol and iso-octane/ethanol blends in a port-fuel injection spark-ignition engine," *Fuel*, vol. 94, pp. 251–261, 2012.

25. N. N. Clark, D. L. M. Jr., T. Klein, and T. S. Higgins, "Quantification of gasoline-ethanol blend emissions effects," *Journal of the Air & Waste Management Association*, vol. 71, no. 1, pp. 3–22, 2021. PMID: 32315258.

26. G. Karavalakis, D. Short, D. Vu, R. Russell, M. Hajbabaei, A. Asa-Awuku, and T. D. Durbin, "Evaluating the effects of aromatics content in gasoline on gaseous and particulate matter emissions from si-pfi and sidi vehicles," *Environmental Science & Technology*, vol. 49, no. 11, pp. 7021–7031, 2015. PMID: 25938171.

27. C. L. Goodfellow, R. A. Gorse, M. J. Hawkins, and J. S. McArragher, "European programme on emissions, fuels and engine technologies (epefe) - gasoline aromatics/e100 study," *SAE Transactions*, vol. 105, pp. 503–526, 1996.

28. E. Zervas, X. Montagne, and J. Lahaye, "Emission of alcohols and carbonyl compounds from a spark ignition engine. influence of fuel and air/fuel equivalence ratio," *Environmental Science & Technology*, vol. 36, no. 11, pp. 2414–2421, 2002. PMID: 12075798.

29. D. Schuetzle, W. O. Siegl, T. E. Jensen, M. A. Dearth, E. W. Kaiser, R. Gorse, W. Kreucher, and E. Kulik, "The relationship between gasoline composition and vehicle hydrocarbon emissions: A review of current studies and future research needs," *Environmental Health Perspectives*, vol. 102, pp. 3–12, 1994.

30. M. Zhang, Y. Ge, X. Wang, H. Xu, J. Tan, and L. Hao, "Effects of ethanol and aromatic compositions on regulated and unregulated emissions of e10-fuelled china-6 compliant gasoline direct injection vehicles," *Renewable Energy*, vol. 176, pp. 322–333, 2021.

31. Z. Tian, W. J. Pitz, R. Fournet, P.-A. Glaude, and F. Battin-Leclerc, "A detailed kinetic modeling study of toluene oxidation in a premixed laminar flame," *Proceedings of the Combustion Institute*, vol. 33, no. 1, pp. 233–241, 2011.

32. S. Namysl, M. Pelucchi, L. Pratali Maffei, O. Herbinet, A. Stagni, T. Faravelli, and F. Battin-Leclerc, "Experimental and modeling study of benzaldehyde oxidation," *Combustion and Flame*, vol. 211, pp. 124–132, 2020.

33. R. Zhu, J. Hu, X. Bao, L. He, and L. Zu, "Effects of aromatics, olefins and distillation temperatures (t50 and t90) on particle mass and number emissions from gasoline direct injection (gdi) vehicles," *Energy Policy*, vol. 101, pp. 185–193, 2017.

34. I. Schifter, L. Díaz, G. Sánchez-Reyna, C. González-Macías, U. González, and R. Rodríguez, "Influence of gasoline olefin and aromatic content on exhaust emissions of 152020.

35. S. White, A. Bajwa, and F. Leach, "Isolated low temperature heat release in spark ignition engines," SAE, 2023.

36. J. Baronick, B. Heller, G. Lach, and H. Luf, "Modal measurement of raw exhaust volume and mass emissions by sesam," *SAE Technical Papers*, 1998.

37. "Automotive fuels-unleaded petrol-requirements and test methods," 2008.

38. X. Wang, J. Gao, Z. Chen, H. Chen, Y. Zhao, Y. Huang, and Z. Chen, "Evaluation of hydrous ethanol as a fuel for internal combustion engines: A review," *Renewable Energy*, vol. 194, pp. 504–525, 2022.

39. Q. Fan, Z. Wang, Y. Qi, S. Liu, and X. Sun, "Research on ethanol and toluene's synergistic effects on auto-ignition and pressure dependences of flame speed for gasoline surrogates," *Combustion and Flame*, vol. 222, pp. 196–212, 2020.

40. V. Shankar, X. Fang, N. Hinton, M. Davy, and F. Leach, "Effect of Ethanol Addition on the Laminar Burning Velocity of Gasoline Surrogates With Toluene," vol. ASME 2022 ICE Forward Conference of *Internal Combustion Engine Division Fall Technical Conference*, 10 2022. V001T02A006.

41. V. Shankar, X. Fang, N. Hinton, M. Davy, and F. Leach, "Effect of ethanol addition on the laminar burning velocities of gasoline surrogates," *Fuel*, vol. 327, p. 125186, 2022.

42. N. Sekularac, X. Fang, V. Shankar, S. Baker, F. Leach, and M. Davy, "Development of a laminar burning velocity empirical correlation for combustion of iso-octane/ethanol blends in air," *Fuel*, vol. 307, p. 121880, 2022.

43. X. Yu, Z. Guo, P. Sun, S. Wang, A. Li, H. Yang, Z. Li, Z. Liu, J. Li, and Z. Shang, "Investigation of combustion and emissions of an si engine with ethanol port injection and gasoline direct injection under lean burn conditions," *Energy*, vol. 189, p. 116231, 2019.

44. P. Dirrenberger, P. Glaude, R. Bounaceur, H. Le Gall, A. P. da Cruz, A. Konnov, and F. Battin-Leclerc, "Laminar burning velocity of gasolines with addition of ethanol," *Fuel*, vol. 115, pp. 162–169, 2014.

45. W. Liu, Y. Qi, R. Zhang, and Z. Wang, "Flame propagation and auto-ignition behavior of iso-octane across the negative temperature coefficient (ntc) region on a rapid compression machine," *Combustion and Flame*, vol. 235, p. 111688, 2022.

ACKNOWLEDGMENTS

Varun Shankar acknowledges the scholarship support of The Rhodes Trust. This publication also arises from research funded by the John Fell Oxford University Press Research Fund.

CONTACT INFORMATION

Felix Leach, Associate Professor
Department of Engineering Science
University of Oxford
Parks Rd
Oxford
OX1 3PJ
UK
felix.leach@eng.ox.ac.uk

DEFINITIONS, ACRONYMS, ABBREVIATIONS

ϕ	fuel-air equivalence ratio
2,4-DNPH	2,4-dinitrophenyl hydrazine
BNC	Berkeley Nucleonics Corporation
CoV	Coefficient of variation
CO	Carbon monoxide
EU	European Union
EVC	Exhaust valve closing
EVO	Exhaust valve opening
FID	Flame ionisation detector
FTIR	Fourier Transform Infrared Spectroscopy
GDI	Gasoline direct injection
GHG	Greenhouse gas
IARC	International agency for research on cancer
IMEP	Indicated mean effective pressure
IVC	Intake valve closing
IVO	Intake valve opening
NMHC	Non-methane hydrocarbon
PFI	Port-fuel injection
PM	Particulate matter
SI	Spark ignition
THC	Total hydrocarbons
TWC	Three-way catalytic converter
UHC	Unburned hydrocarbons
USA	United States of America

APPENDIX A

The measured cylinder pressure profiles for each of the pure, binary, and ternary mixtures are presented at stoichiometric conditions at a speed of 1100 rpm. The cylinder temperature is derived from the cylinder pressure using Equations 1 and 2 assuming ideal gas law and i refers to every 0.1 °CA.

$$m = \frac{P_{inlet} V_{inlet}}{R T_{inlet}} \tag{1}$$

$$T_i = \frac{P_i V_i}{m R} \tag{2}$$

Figure A.1 and A.2 present the measured cylinder pressure and derived temperature profiles, respectively, for the pure fuels of ethanol, toluene, and iso-octane at stoichiometric conditions, speed of 1100 rpm, and a load of 1.80 bar IMEP.

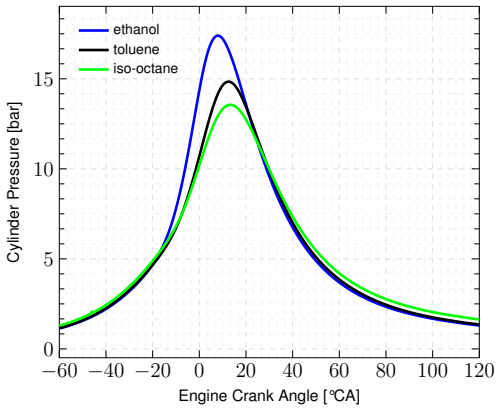

Figure A.1: Measured cylinder pressure profiles for ethanol (blue), toluene (black), and iso-octane (green) averaged over 3 repeats each with 300 cycles at a speed of 1100 rpm, load of 1.80 bar IMEP, and stoichiometric conditions.

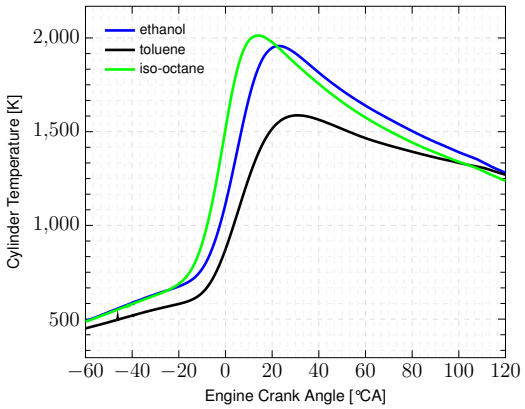

Figure A.2: Calculated cylinder temperature profiles for ethanol (blue), toluene (black), and iso-octane (green) averaged over 3 repeats each with 300 cycles at a speed of 1100 rpm, load of 1.80 bar IMEP, and stoichiometric conditions.

Figure A.3 and A.4 present the measured cylinder pressure and derived temperature profiles, respectively, for the binary mixtures of TE25, TE50, and TE75 at stoichiometric conditions, speed of 1100 rpm, and a load of 1.80 bar IMEP.

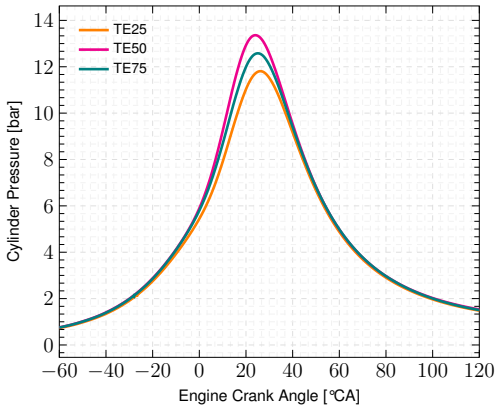

Figure A.3: Measured cylinder pressure profiles for TE25 (orange), TE50 (magenta), and TE75 (teal) averaged over 3 repeats each with 300 cycles at a speed of 1100 rpm, load of 1.80 bar IMEP, and stoichiometric conditions.

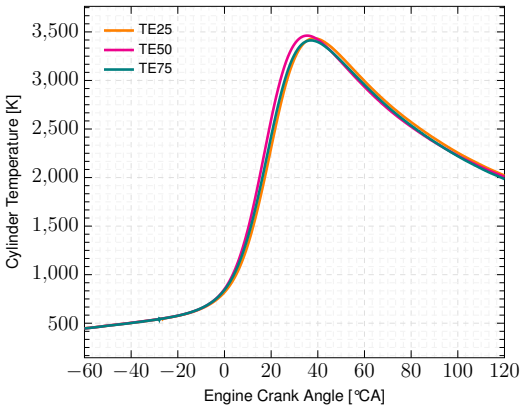

Figure A.4: Calculated cylinder temperature profiles for TE25 (orange), TE50 (magenta), and TE75 (teal) averaged over 3 repeats each with 300 cycles at a speed of 1100 rpm, load of 1.80 bar IMEP, and stoichiometric conditions.

Figure A.5 and A.6 present the measured cylinder pressure and derived temperature profiles, respectively, for the ternary mixtures of OTE25_LowT and OTE25_HighT at stoichiometric conditions, speed of 1100 rpm, and a load of 1.95 bar IMEP.

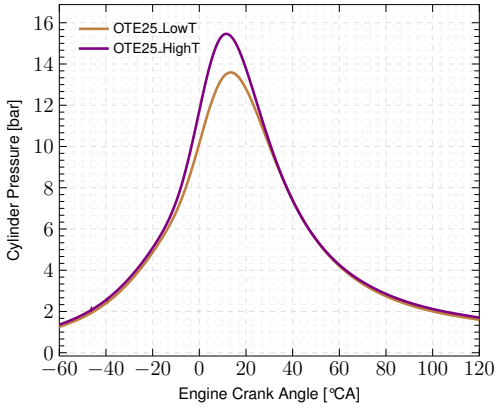

Figure A.5: Measured cylinder pressure profiles for OTE25_LowT (brown) and OTE25_HighT (violet) averaged over 3 repeats each with 300 cycles at a speed of 1100 rpm, load of 1.95 bar IMEP, and stoichiometric conditions.

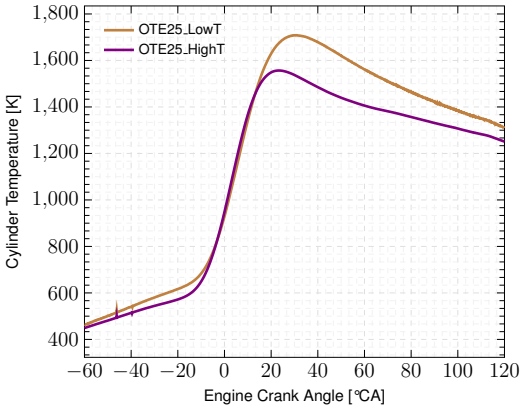

Figure A.6: Calculated cylinder temperature profiles for OTE25_LowT (brown) and OTE25_HighT (violet) averaged over 3 repeats each with 300 cycles at a speed of 1100 rpm, load of 1.95 bar IMEP, and stoichiometric conditions.

Figure A.5 and A.6 present the measured cylinder pressure and derived temperature profiles, respectively, for the ternary mixtures of OTE25_LowT and OTE25_HighT at stoichiometric conditions, speed of 1100 rpm, and a load of 3.00 bar IMEP.

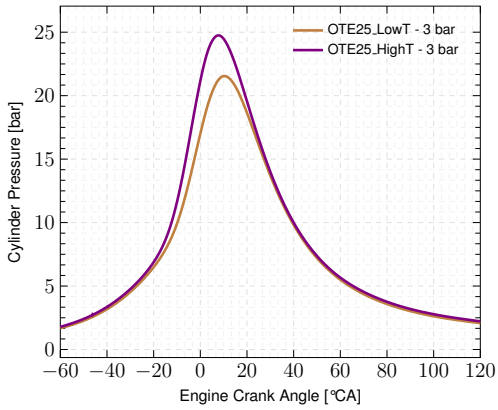

Figure A.7: Measured cylinder pressure profiles for OTE25_LowT (brown) and OTE25_HighT (violet) averaged over 3 repeats each with 300 cycles at a speed of 1100 rpm, load of 3.00 bar IMEP, and stoichiometric conditions.

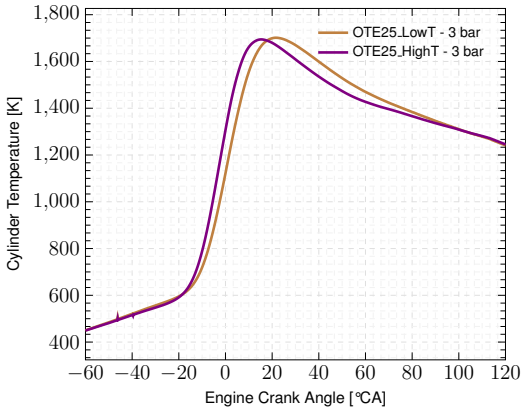

Figure A.8: Calculated cylinder temperature profiles for OTE25_LowT (brown) and OTE25_HighT (violet) averaged over 3 repeats each with 300 cycles at a speed of 1100 rpm, load of 3.00 bar IMEP, and stoichiometric conditions.